Superoptimal charging of quantum batteries via reservoir engineering: Arbitrary energy transfer unlocked

Borhan Ahmadi,[1,*] Paweł Mazurek,[2,†] Shabir Barzanjeh,[3] and Paweł Horodecki[1]

[1] *International Centre for Theory of Quantum Technologies, University of Gdansk, Jana Bażyńskiego 1A, Gdansk 80-309, Poland*

[2] *Institute of Informatics, Faculty of Mathematics, Physics and Informatics, University of Gdańsk, Wita Stwosza 63, Gdańsk 80-308, Poland*

[3] *Department of Physics and Astronomy, University of Calgary, Calgary, Alberta T2N 1N4, Canada*

(Received 29 July 2024; revised 7 January 2025; accepted 21 January 2025; published 4 February 2025)

Arbitrary energy transfer is only feasible in nondissipative charger-battery systems; in realistic processes, however, energy dissipation prevents this. In this work, we introduce a novel charging technique in which the coherent charger-battery interaction is replaced by a dissipative interaction via an engineered reservoir. We demonstrate that exploiting the collective effects of the engineered reservoir allows for additional optimization, giving rise to an optimal redistribution of energy. This not only significantly enhances the efficiency of the charging process but also remarkably enables the quantum battery to accumulate unlimited energy—limited only by the natural energy scale of the device. This phenomenon cannot occur in conventional charger-battery schemes. The article unveils the intricacies of built-in detuning within the context of a shared environment, offering a deeper understanding of the charging mechanisms involved. These findings apply naturally to quantum circuit battery architectures, suggesting the feasibility of efficient energy storage in these systems. The superoptimal charging mechanism offers a practical avenue for boosting the capacity of the battery through charger-battery configurations.

DOI: 10.1103/PhysRevApplied.23.024010

I. INTRODUCTION

The role of energy transfer is of primary importance in industry. In recent years, significant research has been devoted to examining how to efficiently facilitate energy transfer between two quantum systems by means of a direct interaction between them in various contexts such as quantum heat engines, quantum thermal logic gates, quantum thermal transistors, quantum switches, and quantum batteries [1–10]. Quantum batteries, a concept introduced in Ref. [11], represent a cutting-edge advancement in the field of energy transfer and storage, leveraging the principles of quantum mechanics to potentially revolutionize energy capture and storage in quantum devices [4,7,8,11–20]. Unlike traditional batteries, quantum batteries use quantum phenomena such as entanglement, coherence and correlations [7,8,12,21–24] to facilitate energy storage processes that could surpass the limitations of conventional systems. We refer the reader to Refs. [13,14,18,25–47] for the newest developments in the field. In particular, Ref. [48] introduced a setting in which a battery is coupled to a charging laser pulse through another quantum system—a charger—with the aim of improving charging properties.

While these contributions have significantly advanced our understanding of quantum batteries, the search for enhanced efficiency drives us to explore new avenues for improving energy storage, most notably boosting its energetic efficiency and power. A novel approach to optimizing the efficiency of quantum battery charging leverages reservoir engineering to induce nonreciprocity [49–61] which, as recently shown, can significantly boost energy transfer to the battery [62]. Reservoir engineering, a crucial technique in quantum technology, involves the deliberate design and manipulation of a system's interaction with its environment to achieve specific quantum states or dynamics [49,58–61].

In this work, we identify a scenario in which reservoir engineering lifts a fundamental limitation of dissipative charger-battery systems (see Fig. 1). In conventional quantum battery charging processes, *unlimited* energy transfer is impossible unless the system is entirely free from dissipation, as dissipation typically limits the amount of energy that can be stored. Here, we demonstrate that by employing reservoir engineering to establish a dissipative interaction, this restriction can be overcome by allowing the quantum battery to accumulate unlimited energy. We begin

*Contact author: borhan.ahmadi@ug.edu.pl, b.ahmadi19@gmail.com

†Contact author: pawel.mazurek@ug.edu.pl

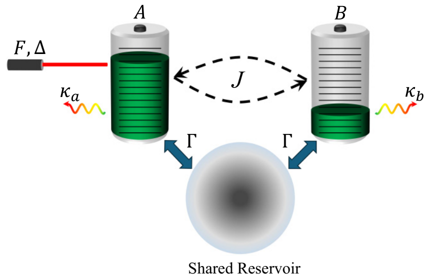

FIG. 1. Schematic representation of the charging process. A quantum charger A coherently interacts with a quantum battery B with a coupling rate J. Both the charger and the battery decay into a shared reservoir at the decay rate Γ, establishing an effective dissipative interaction between them. A laser field with amplitude F is used to supply energy to the charger. Here, κ_a and κ_b describe the local damping rates of each mode.

by showing that optimal charging for any charging process is achieved by optimizing the characteristics of the external energy source for a given charging device, which is governed by a built-in detuning of the charger-battery structure. We then show that the engineered shared reservoir allows for *further* optimization of the charging process over the internal structure of the charging device (the parameters of the coupling with the engineered reservoir), resulting in *superoptimal* charging. Generally, creating coherent interaction is more challenging than designing broadband lossy systems. Finally, we show that superoptimal charging allows for the energy of the battery in the charger-battery setting to exceed that of the battery directly coupled to the external laser (with no charger mediating the process), providing justification for charger-battery configurations [48]. This research opens up new avenues for exploring chiral and topological properties in systems making use of dissipative coupling.

II. QUANTUM BATTERY MODEL

Figure 1 shows a schematic of the system in a charger-battery configuration [48], including a harmonic oscillator serving as the charger with a resonance frequency of ω_a and a local damping rate κ_a. This charger interacts with another mode acting as the battery, characterized by a frequency of ω_b and a damping rate κ_b. The coherent interaction between the charger and the battery is described by $J = |J|e^{i\phi}$. An external classical drive with frequency ω_L and amplitude F provides energy to the charger during the charging process. The Hamiltonian describing this driven bipartite system AB can be written, in the rotating frame with respect to ω_L, as

$$H = H_{AB} + H_L. \tag{1}$$

The Hamiltonian H_{AB} is given by $H_{AB} = H_a + H_b + H_{\text{int}}$, where $H_a = \Delta a^\dagger a$ ($\hbar = 1$) and $H_b = \Delta b^\dagger b$ represent the free Hamiltonians of the charger and the battery, respectively. Here, a (b) and $a^\dagger$ ($b^\dagger$) are the annihilation and creation operators of the charger (battery), and $\Delta = \omega_L - \omega$ denotes the local detuning of the input laser beam from the optical charger resonance frequency. For simplicity, we assume that the charger and the battery are in resonance, i.e., $\omega_a = \omega_b = \omega$. The interaction Hamiltonian, H_{int}, is described as $Ja^\dagger b + J^* ab^\dagger$, and the term $H_L = F(e^{i\Delta t}a + e^{-i\Delta t}a^\dagger)$ accounts for the laser field applied to the charger for feeding energy into the system (under the rotating-wave approximation [63]). As we construct our charging system AB, the *built-in* eigenfrequencies of the Hamiltonian H_{AB} are established as $\omega_\pm = \omega \pm |J|$ (see Appendix A 1). This, in turn, creates a built-in detuning of $\Delta_{\text{in}} = \pm|J|$, where the subscript in indicates its built-in origin. This suggests that in a *nondissipative* charging process, to optimize energy transfer to the battery, the detuning of the external field Δ should be equal to this built-in detuning Δ_{in}. This phenomenon will be rigorously proved in the following sections. In addition, we also consider a dissipative interaction between the charger and the battery, mediated by their mutual coupling to a shared reservoir characterized by a coupling rate of Γ. This interaction is realized by adiabatically eliminating the reservoir's degrees of freedom. From a practical perspective, the shared reservoirs could be an additional damped cavity or a waveguide [51,64]. The dynamics of the system can be described by the Lindblad master equation [51]

$$\dot{\rho} = -i[H, \rho] + \Gamma\mathcal{D}_z[\rho] + \kappa_a\mathcal{D}_a[\rho] + \kappa_b\mathcal{D}_b[\rho], \tag{2}$$

where $\mathcal{D}_O[\cdot] = O \cdot O^\dagger - \frac{1}{2}\{O^\dagger O, \cdot\}$ represents the dissipative superoperator resulting from the coupling to the reservoirs. It is the second term in Eq. (2) that represents the dissipation of both modes into the shared reservoir, resulting in dissipative coupling between the two modes. Here, Γ corresponds to the rate at which a photon is absorbed and emitted by the common reservoir due to this coupling, while $z = p_a a + p_b b$, with p_a and p_b following the normalization condition $|p_b p_a^*| = 1$. The latter two terms account for local damping of each of the modes due to their coupling ports to the surrounding environment [51,65], with κ_a and κ_b being the rates of the corresponding excitation and relaxation processes. As we are going to explore, in the presence of dissipation, the optimal detuning is no longer the built-in detuning but also includes corrections depending on the type of dissipation.

We define the internal energy of each subsystem as $E_i = \omega\text{tr}\left[\rho_i i^\dagger i\right]$ with $i = a, b$ [66]. Given the assumption of zero temperature for all reservoirs, the states of subsystems remain pure if the initial state of the entire system is a pure product state [67]. This, in turn, implies that all the internal energy of the battery can be extracted as ergotropy [68]. Therefore, in the following, we will only discuss the internal energies of the battery and the charger.

III. OPTIMAL CHARGING

The local dynamics of the system are described by a set of differential equations of motion for the evolution of the first and second moments (see Appendix A 2), and the energy of the charger and the battery in the steady state are calculated as

$$E_A = \frac{4F^2\mathcal{K}_{bb}}{|\mathcal{J}(i\Gamma,\phi) - \mathcal{K}_{ab}|^2}, \tag{3}$$

$$E_B = \frac{4F^2\mathcal{J}(\Gamma,\alpha)}{|\mathcal{J}(i\Gamma,\phi) - \mathcal{K}_{ab}|^2}, \tag{4}$$

where $\mathcal{K}_{bb} = 4\Delta^2 + (\Gamma_b + \kappa_b)^2$, $\mathcal{K}_{ab} = \big(2\Delta + i(\Gamma_a + \kappa_a)\big)\,(2\Delta + i(\Gamma_b + \kappa_b))$, $\mathcal{J}(x,\theta) = 4|J|^2 + x^2 - 4|J|x\cos\theta$, and $\alpha + \phi = \pi/2$. From Eqs. (A19)–(A23) of Appendix A 2, we can see that $\mathcal{J}(x,\theta)$ effectively incorporates the interactions facilitating energy transfer between the charger and the battery, while $\mathcal{K}_{ij}$ describes processes restricting energy transfers, such as energy dissipation or detuning. We first start the analysis by examining the conventional quantum battery scenario (the absence of the shared reservoir), which is achieved by setting $\Gamma = 0$. We select the initial states of both the charger and battery to be ground states. It is worth mentioning here that since the evolution of the system in our work is Markovian, the energy of the final state is invariant for various initial states. In the ideal charging process, in which there are no local dissipations (i.e., $\kappa_a = \kappa_b = 0$), by optimizing E_B over Δ, we find that the optimal detuning equals the built-in detuning: $\Delta_{\rm opt} = \Delta_{\rm in}$. In fact, in the case $\Delta = \Delta_{\rm in}$, we have $\mathcal{J}(i\Gamma,\phi) = \mathcal{K}_{ab}$, which gives rise to *unlimited* energy transfer to the battery. This phenomenon of unlimited energy transfer indicates the crucial significance of the built-in detuning $\Delta_{\rm in}$; however, in realistic charging processes, local dissipations are inevitable. Therefore, for nonzero local dissipation rates $\kappa_{a(b)}$, optimizing E_B over Δ, the optimal charging process results in

$$\Delta_{\rm opt} = \pm\sqrt{\Delta_{\rm in}^2 - \frac{\kappa^2}{8}}, \tag{5}$$

where $\kappa^2 = \kappa_a^2 + \kappa_b^2$. Note that in this case, arbitrary (unlimited) energy transfer to the battery is not feasible even if the battery is perfectly insulated, i.e., $\kappa_b = 0$. This is because the dissipation on the charger, κ_a, still causes the energy of the battery to saturate after some time. This can be seen from the denominator in Eq. (4) which takes the form $|4J^2 - (2\Delta + i\kappa_a)(2\Delta + i\kappa_b)|^2$. This is always greater than zero due to the imaginary terms resulting from local dissipation rates $\kappa_{a(b)}$. It is also worth mentioning that Eq. (5) implies that in an experiment, one needs to measure the dissipation rates to perform the optimal charging process. In Fig. 4, we plot the time evolution of $E_B(t)$ for the optimal charging procedure (dashed blue line). Additionally, in Fig. 4, we illustrate $E_B(t)$ for a nonoptimal detuning case (green solid line) by taking $\Delta = 0$, to underscore the substantial influence of optimal detuning on the charging process.

It is worth mentioning that Eq. (5) implies the important fact that the charging laser field comprehensively perceives not only the coherent interaction J, but also energy dumping to the local baths. The interactions with the baths show their effects via the dissipation rates $\kappa_{a(b)}$. Therefore, in presence of local dissipations, κ is in fact the correction to the built-in detuning $\Delta_{\rm in}$ (a fact overlooked in our earlier work [18]). In other words, the optimal detuning is influenced by the entirety of the interactions. We also notice that in the conventional scenario $\Delta_{\rm opt}$ depends only on the strength of the coherent interaction, and not on its phase ϕ.

IV. SUPEROPTIMAL CHARGING

Here we demonstrate that *replacing* the coherent interaction with the shared reservoir allows for *significant outperformance* of the optimal conventional charging process. In Appendix A 3 we also show that the simple *addition* of the common reservoir to the scheme does not offer a straightforward advantage. To better understand the mechanism, we first provide insight into the microscopic dynamics underlying the concept of superoptimal charging by examining the master equation [Eq. (2)] and then introduce our approach aimed at surpassing the optimal conventional charging strategy discussed in the previous section. Equation (2) may be recast as follows:

$$\begin{aligned}\dot\rho = &-i[H,\rho] + (\Gamma_a + \kappa_a)\mathcal{D}_a[\rho] + (\Gamma_b + \kappa_b)\mathcal{D}_b[\rho] \\ &+ \Gamma\mathcal{D}_a^b[\rho] + \Gamma\mathcal{D}_b^a[\rho],\end{aligned} \tag{6}$$

where $\Gamma_i = \Gamma|p_i|^2$ with $i = a,b$ and $\mathcal{D}_x^y[\cdot] =: x\cdot y^\dagger - \frac{1}{2}\{x^\dagger y,\cdot\}$. Equation (6) implies that the shared reservoir dissipator $\mathcal{D}_z[\rho]$ from Eq. (2) in practice affects the charging process in two distinct manners: firstly, via $\Gamma_x\mathcal{D}_x[\rho]$, it causes energy dissipation of the charger and the battery into the shared reservoir at rates Γ_a and Γ_b, respectively; secondly, via $\Gamma\mathcal{D}_x^y[\rho]$, it facilitates energy exchange between the charger and the battery at rate Γ. Therefore, $\Gamma\mathcal{D}_x^y[\rho]$ provides a dissipative interaction between the charger and the battery, paving the way for more transfer of energy. Notably, even with the direct coherent coupling turned off ($J = 0$), energy exchange still remains feasible through the shared reservoir with rate Γ. Note that in quantum optics, the same generator of the form Eq. (6) is also used to explain the phenomenon of collective resonance fluorescence [69].

A comparison between the two charging scenarios, the dissipative and the coherent one, will be performed while keeping the parity $\Gamma = 2|J|$ between the coupling rates. This ensures comparable instantaneous charging power in both approaches, as suggested by the equations of motion [see Eqs. (A19)–(A23) in Appendix A 2]. Here, the transfer of energy from the charger to the battery is governed by the strength of interaction J and a factor of absorption/emission photon rate from the common reservoir $\Gamma/2$, respectively. Under the constraint of comparable instantaneous charging power, we will show that higher levels of energy in the battery can be achieved due to the dissipative coupling. As a further justification, we add that we actually expect designing and operating dissipative broadband lossy systems to be easier than the coherent setups.

The solution for dissipation-assisted charging is obtained by setting $J=0$ in the equations of motion. From Eqs. (3) and (4) it can be shown that in this scenario, the optimal detuning is zero, $\Delta_{\rm opt}=0$ [see also Eq. (A16) of Appendix A 1]. In Fig. 2, we present a plot depicting the battery energy for $\Gamma=0.4$, $J=0$, and $\Delta_{\rm opt}=0$, comparing it with the optimal conventional scenario in which $|J|=0.2$. Clearly, dissipative charging does not provide any advantage. We should stress that in Fig. 2 and the subsequent figures, energy is plotted against Jt, where the scaling factor J is taken from the conventional scenario.

As we show below, leveraging the structure brought about by the engineered reservoir, we are able to optimize the process by manipulating the relative values of $\Gamma_{a(b)}$. Examining the equations of motion, we see that changing Γ_a and Γ_b by altering p_a and p_b can affect the energy of the charger and the battery. Defining the ratio $y=|p_a|^2/|p_b|^2$, we then have $\Gamma_a/\Gamma_b=y$. Now, rewriting Eqs. (3) and (4) as functions of y, we find that both the total energy of the entire setup and the energy of the battery are optimized for $y=\sqrt{\kappa_a/\kappa_b}$, while the energy of the charger reaches its maximum in the limit $y\to 0$. We see that the essence of the optimization is to properly reflect the imbalance between the local dissipation strengths $\kappa_{a(b)}$ in the ratio of $p_{a(b)}$. Consequently, we will refer to this as a *superoptimal* charging process in a scenario with a shared reservoir optimized in this way. The corresponding superoptimal stationary energies are given by

$$E^S_{A,\text{sup-opt}}=\frac{4F^2\left(\Gamma+\sqrt{\kappa_a\kappa_b}\right)^2}{\kappa_a^2\left(2\Gamma+\sqrt{\kappa_a\kappa_b}\right)^2}, \tag{7}$$

$$E^S_{B,\text{sup-opt}}=\frac{4\Gamma^2F^2}{\kappa_a\kappa_b\left(2\Gamma+\sqrt{\kappa_a\kappa_b}\right)^2}, \tag{8}$$

$$\xi^S_{\text{sup-opt}}=\frac{4F^2\left(\kappa_a\kappa_b^2+2\Gamma\kappa_b\sqrt{\kappa_a\kappa_b}+\Gamma^2(\kappa_a+\kappa_b)\right)}{\kappa_a^2\kappa_b\left(2\Gamma+\sqrt{\kappa_a\kappa_b}\right)^2}, \tag{9}$$

where the superscript S denotes the presence of the shared reservoir and $\xi\equiv E_A+E_B$ denotes the total energy within the entire system. As a direct result of the optimization, we observe a significant increase in the total energy of the system ξ^S (see Appendix A 4). This indicates that the optimization helps to preserve more energy in the charger-battery system against the dissipation. Furthermore, the second intriguing result, as detailed below, is that optimization not only enhances the total energy within the entire system but also allows for channeling, in the most efficient way, the energy into the battery B. It is worth noting that the zero optimal detuning in superoptimal charging is in fact another advantage of the superoptimal configuration since it is experimentally more convenient. In the conventional optimal charging protocol, one needs to measure the interaction coupling J and the local dissipation rates $\kappa_{a(b)}$ to compute the optimal detuning for performing the optimal charging process; in contrast, for the superoptimal configuration, one simply needs to match the laser field frequency with that of the charger, making the process significantly easier for experimentation.

As shown in Fig. 3(a), applying further optimization through manipulation of $\Gamma_{a(b)}$ in the charging process causes $E^S_{A,\text{sup-opt}}$ to be substantially lower than $E_{A,\rm opt}$, emphasizing again the significant benefits of having an engineered reservoir in the charging process. At the same time, as shown in Fig. 3(b), we can observe that the super-optimized energy of the battery $E^S_{B,\text{sup-opt}}$ (solid red line) significantly surpasses the optimal conventional energy $E_{B,\rm opt}$. This further justifies the name *superoptimal* charging process, since it outperforms the optimal conventional charging process. Comparing Fig. 2(a) with Fig. 3(a) and Fig. 2(b) with Fig. 3(b), the remarkable phenomenon that we observe is the redistribution of the total energy within the entire system due to optimization, with a notable increase in energy in the desired location—namely, the battery B.

The most significant result of our work is as follows. In conventional settings, whenever there is dissipation in the charging system, it becomes impossible to transfer an arbitrary amount of energy to the battery; the energy transfer is limited by the dissipation, even if the battery itself is perfectly insulated from dissipation (i.e., $\kappa_b=0$). As can be observed from Eq. (4), dissipation on the charger side alone ($\kappa_a\neq 0$) is sufficient to prevent *unlimited* energy transfer to the battery. This restriction is remarkably lifted using reservoir engineering. The optimization freedom provided by reservoir engineering allows for this remarkable phenomenon, as demonstrated in Eq. (8). By insulating only one of either the charger or the battery, it becomes possible to transfer an arbitrary amount of energy to the battery. This implies that as long as the battery remains connected to the charger, it continues to accumulate more and more energy over time. In other words, superoptimal charging *unlocks* the arbitrary energy transfer (see Appendix A 5 for further details). We stress that the redistribution gap caused by the engineered shared reservoir

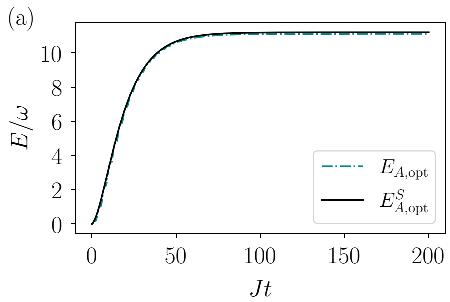

FIG. 2. Energies of (a) the charger E_A and (b) the battery E_B vs Jt for the optimal conventional scenario and the shared-reservoir-assisted scenario. In the conventional scenario, we have $F = 0.1$ and $|J| = 0.2$. In the shared-reservoir-assisted scenario, $F = 0.1$, $J = 0$, $\Gamma = 0.4$, $p_a = 1$, and $p_b = 1$. In both procedures, we have $\kappa_a = 0.05$ and $\kappa_b = 0.01$, and the corresponding optimal detuning Δ_{opt}.

$\mathcal{G}^r_B \equiv E^S_{B,\text{sup-opt}} - E_{B,\mathrm{opt}}$ is always positive (see Appendix A 6 and Appendix A 7 for further discussion).

We shall briefly discuss other features of the dissipative charging method. Dissipative charging has less stability with respect to detuning deviations as compared to conventional coherent charging (see Appendix A 8 for details).

We conclude with providing a positive answer to a question about the justification for adding a charger to intermediate between the battery and the charging field. Through a detailed study (see Appendix A 9) we show that replacing the coherent charger-battery interaction with a dissipative one enables higher levels of energy to be stored in the battery, as compared to direct charging, thus unlocking the benefits of the charger-battery configuration.

V. SUMMARY AND OUTLOOK

In this work, we investigate the protocol for unlocking arbitrary energy transfer in a dissipative charger-battery system. We begin by optimization of the external energy source (its frequency) by examining the built-in detunings of the charging setup. We then move to setups that introduce an engineered reservoir into the charging processes. Our investigation reveals that replacing the coherent interaction with a dissipative interaction via an engineered shared reservoir not only reproduces the same optimal charging outcomes but also allows for further optimization over the internal structure of the charging device (the parameters of the coupling with the engineered reservoir), giving rise to superoptimal charging. As a result, we observe that not only does the total energy within the entire system attain a higher value in the steady state, but also that a beneficial redistribution of energy occurs within the charger-battery system, with a notable increase of energy in the desired location—namely, the battery—presenting a significant advancement in quantum battery charging. This advantage is observable even in the transient regime. Above all, we show that the ultimate advantage of an engineered reservoir lies in its ability to facilitate arbitrary energy transfer to the battery, which is impossible in conventional charging processes. Therefore, we conclude that the superoptimal charging, achieved through careful optimization of the engineered reservoir, paves the way for

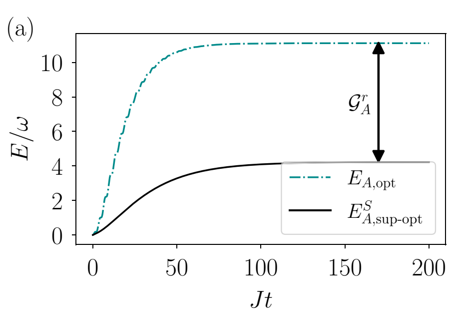

FIG. 3. Energies of (a) the charger E_A and (b) the battery E_B vs Jt for the optimal conventional scenario and the shared-reservoir-assisted scenario. Here, $\mathcal{G}^r_{A(B)}$ quantifies the redistribution gap caused by the engineered shared reservoir. For the conventional scenario, we have $F = 0.1$ and $|J| = 0.2$. For the shared-reservoir-assisted scenario $F = 0.1$, $J = 0$, $\Gamma = 0.4$, $p_a = (\kappa_a/\kappa_b)^{1/4}$, and $p_b = (\kappa_a/\kappa_b)^{-1/4}$. In both procedures, we chose $\kappa_a = 0.05$ and $\kappa_b = 0.01$, and the corresponding optimal detuning Δ_{opt}.

transformative developments in high-performance energy solutions, in particular in charger-battery configurations.

ACKNOWLEDGMENTS

B.A. acknowledges support from the National Science Center, Poland, within the QuantERA II Programme (Grant No. 2021/03/Y/ST2/00178, acronym ExTRaQT), which has received funding from the European Union's Horizon 2020 program. B.A. also acknowledges Robert Alicki for helpful discussions. S.B. acknowledges funding by the Natural Sciences and Engineering Research Council of Canada (NSERC) through its Discovery Grant, funding and advisory support provided by Alberta Innovates through the Accelerating Innovations into CarE (AICE) – Concepts Program, and support from Alberta Innovates and NSERC through Advance Grant.

APPENDIX

1. Global View Analysis

To have a global understanding of the dynamics of the charging process, we rewrite the system Hamiltonian as

$$H = \omega_A a^\dagger a + \omega_B b^\dagger b + (J a^\dagger b + J^* b^\dagger a) + F(e^{i\omega_L t} a + e^{-i\omega_L t} a^\dagger) \tag{A1}$$

in the properly selected basis, which depends on the value of J. We introduce supermode the operators

$$C_+ = \frac{a + e^{i\phi} b}{\sqrt{2}}, \tag{A2}$$

$$C_- = \frac{a - e^{i\phi} b}{\sqrt{2}}, \tag{A3}$$

with eigenfrequencies $\omega_\pm = \omega \pm |J|$, which satisfy the commutation relations $[C_+, C_-] = [a, b] = 0$ and $[C_\pm, C_\pm^\dagger] = [a, a^\dagger] = [b, b^\dagger] = 1$. We make $C_\pm$ depend on the phase of the coupling $J = |J| e^{i\phi}$. From Eqs. (A2) and (A3), we have

$$a = \frac{C_+ + C_-}{\sqrt{2}}, \tag{A4}$$

$$b = e^{-i\phi} \frac{C_+ - C_-}{\sqrt{2}}, \tag{A5}$$

and hence we obtain

$$\begin{aligned} H = {} & (\Delta + |J|)\, C_+^\dagger C_+ + (\Delta - |J|)\, C_-^\dagger C_- \\ & + \frac{F}{\sqrt{2}} \left(e^{i\omega_L t} C_+ + e^{-i\omega_L t} C_+^\dagger \right) \\ & + \frac{F}{\sqrt{2}} \left(e^{i\omega_L t} C_- + e^{-i\omega_L t} C_-^\dagger \right). \end{aligned} \tag{A6}$$

At the same time, the master equation given in Eq. (2) of the main text can be rewritten as

$$\dot{\rho} = -i[H, \rho] + \Gamma \mathcal{D}_z[\rho] + \kappa_a \mathcal{D}_{z_a}[\rho] + \kappa_b \mathcal{D}_{z_b}[\rho], \tag{A7}$$

where

$$z_a =: p_a^a C_+ + p_b^a C_-, \tag{A8}$$

with $p_a^a = \frac{1}{\sqrt{2}}, p_b^a = \frac{1}{\sqrt{2}}$ based on Eq. (A4),

$$z_b =: p_a^b C_+ + p_b^b C_-, \tag{A9}$$

with $p_a^b = e^{-i\phi}/\sqrt{2}$, $p_b^b = -e^{-i\phi}/\sqrt{2}$ based on Eq. (A5), and

$$z = p_a \frac{C_+ + C_-}{\sqrt{2}} + p_b e^{-i\phi} \frac{C_+ - C_-}{\sqrt{2}} = p_a^z C_+ + p_b^z C_-. \tag{A10}$$

In the basis defined by $p_a^z = (p_a + e^{-i\phi} p_b)/\sqrt{2}$ and $p_b^z = (p_a - e^{-i\phi} p_b)/\sqrt{2}$, it is evident that the local dissipators $\mathcal{D}_a$ and $\mathcal{D}_b$, expressed in the basis of a and b, consistently translate into the global dissipators $\mathcal{D}_{z_a}$ and $\mathcal{D}_{z_b}$ in the new basis. Conversely, by setting $p_a = \pm p_b e^{-i\phi}$, we ensure that the dissipator $\mathcal{D}_z$, which is global in the basis of a and b, becomes local in the basis of $C+$ and C_-.

To formulate the equations of motion in the basis of C_+ and C_-, we introduce $\mu_z = -p_a^z (p_b^z)$, $\mu_a = -p_a^a (p_b^a) = -\frac{1}{2}$, and $\mu_b = -p_a^b (p_b^b)^* = \frac{1}{2}$. Subsequently, leveraging the linearity of the master equation and accounting for the adjusted amplitudes F associated with both degrees of freedom, we arrive at

$$\begin{aligned} \frac{d\langle C_+ \rangle}{dt} = {} & -\frac{\Gamma |p_a^z|^2 + \frac{\kappa_a + \kappa_b}{2} + 2i(\Delta + |J|)}{2} \langle C_+ \rangle \\ & + \left(\frac{\Gamma}{2} \mu_z^* + \frac{\kappa_b - \kappa_a}{4} \right) \langle C_- \rangle - i \frac{F}{\sqrt{2}}, \end{aligned} \tag{A11}$$

$$\begin{aligned} \frac{d\langle C_- \rangle}{dt} = {} & -\frac{\Gamma |p_b^z|^2 + \frac{\kappa_a + \kappa_b}{2} + 2i(\Delta - |J|)}{2} \langle C_- \rangle \\ & + \left(\frac{\Gamma}{2} \mu_z + \frac{\kappa_b - \kappa_a}{4} \right) \langle C_+ \rangle - i \frac{F}{\sqrt{2}}, \end{aligned} \tag{A12}$$

$$\begin{aligned} \frac{d\langle C_+^\dagger C_+ \rangle}{dt} = {} & -\left(\Gamma |p_a^z|^2 + \frac{\kappa_a + \kappa_b}{2} \right) \langle C_+^\dagger C_+ \rangle \\ & + 2\Re \left\{ \left(\frac{\Gamma}{2} \mu_z^* + \frac{\kappa_b - \kappa_a}{4} \right) \langle C_+^\dagger C_- \rangle \right\} \\ & - 2\Im \left\{ \frac{F}{\sqrt{2}} \langle C_+ \rangle \right\}, \end{aligned} \tag{A13}$$

$$\frac{d\langle C_-^\dagger C_-\rangle}{dt} = -\left(\Gamma|p_b^z|^2 + \frac{\kappa_a+\kappa_b}{2}\right)\langle C_-^\dagger C_-\rangle + 2\Re\left\{\left(\frac{\Gamma}{2}\mu_z^* + \frac{\kappa_b-\kappa_a}{4}\right)\langle C_+^\dagger C_-\rangle\right\} - 2\Im\left\{\frac{F}{\sqrt{2}}\langle C_-\rangle\right\}, \quad \text{(A14)}$$

$$\frac{d\langle C_+^\dagger C_-\rangle}{dt} = -\frac{\Gamma(|p_a^z|^2+|p_b^z|^2)+\kappa_a+\kappa_b-4i|J|}{2}\langle C_+^\dagger C_-\rangle + \left(\frac{\Gamma}{2}\mu_z + \frac{\kappa_b-\kappa_a}{4}\right)\langle C_+^\dagger C_+\rangle + \left(\frac{\Gamma}{2}\mu_z + \frac{\kappa_b-\kappa_a}{4}\right)\langle C_-^\dagger C_-\rangle - i\frac{F}{\sqrt{2}}\langle C_+\rangle + i\frac{F}{\sqrt{2}}\langle C_-\rangle. \quad \text{(A15)}$$

By selecting $\phi = 0$, the expressions for p_a^z and p_b^z become $p_a^z = (p_a + p_b)/\sqrt{2}$ and $p_b^z = (p_a - p_b)/\sqrt{2}$. Specifically, when $p_a = p_b$, we obtain $p_a^z = p_a$ and $p_b^z = 0$, resulting in $\mu_z = 0$. Referring to Eq. (A14), this implies that the global mode C_- experiences a decoherence-free evolution concerning the shared reservoir, mimicking a scenario with no shared reservoir. Conversely, by choosing $\phi = \pi$, it is the global mode C_+ that experiences a decoherence-free evolution concerning the shared reservoir.

For $\phi \neq 0$, the correction to the built-in detuning is more complicated due to the presence of the shared reservoir:

$$\Delta_{\text{opt}} = -\frac{6^{1/3}\left(8\Delta_{\text{in}}^2 - 2\Gamma^2 - \Gamma_a^2 - \Gamma_b^2 - 2\Gamma_a\kappa_a - \kappa_a^2 - 2\Gamma_b\kappa_b - \kappa_b^2\right)}{2\times 6^{2/3}(K-M)^{1/3}} - \frac{(K-M)^{2/3}}{2\times 6^{2/3}(K-M)^{1/3}}, \quad \text{(A16)}$$

where

$$K =: 36|J|\Gamma\cos\phi\,(\Gamma_a+\Gamma_b+\kappa_a+\kappa_b), \quad \text{(A17)}$$

$$M =: 6^{1/2}\Big(\big(8\Delta_{\text{in}}^2 - 2\Gamma^2 - \Gamma_a^2 - \Gamma_b^2 - 2\Gamma_a\kappa_a - \kappa_a^2 - 2\Gamma_b\kappa_b\kappa_b^2\big)^3 - 216\Delta_{\text{in}}^2\Gamma^2(\Gamma_a - \Gamma_b - \kappa_a - \kappa_b)^2\cos\phi^2\Big)^{1/2}. \quad \text{(A18)}$$

Setting $\Gamma = 0$, we obtain the optimal detuning given in Eq. (5) of the main text.

2. Charging Dynamics

The local dynamics of the system are described by exploiting the master equation [Eq. (2) in the main text]. The evolution of the first and second moments is given by

$$\frac{d\langle a\rangle}{dt} = -\frac{\Gamma_a+\kappa_a+2i\Delta}{2}\langle a\rangle - i\left(J + i\mu\frac{\Gamma}{2}\right)\langle b\rangle - iF, \quad \text{(A19)}$$

$$\frac{d\langle b\rangle}{dt} = -\frac{\Gamma_b+\kappa_b+2i\Delta}{2}\langle b\rangle - i\left(J^* + i\mu^*\frac{\Gamma}{2}\right)\langle a\rangle, \quad \text{(A20)}$$

$$\frac{d\langle a^\dagger a\rangle}{dt} = -(\Gamma_a+\kappa_a)\langle a^\dagger a\rangle - 2\Re\left\{i\left(J + i\mu\frac{\Gamma}{2}\right)\langle a^\dagger b\rangle\right\} - 2F\Im\{\langle a\rangle\}, \quad \text{(A21)}$$

$$\frac{d\langle b^\dagger b\rangle}{dt} = -(\Gamma_b+\kappa_b)\langle b^\dagger b\rangle + 2\Re\left\{i\left(J - i\mu\frac{\Gamma}{2}\right)\langle a^\dagger b\rangle\right\}, \quad \text{(A22)}$$

$$\frac{d\langle a^\dagger b\rangle}{dt} = -\frac{\Gamma_a+\kappa_a+\Gamma_b+\kappa_b}{2}\langle a^\dagger b\rangle - i\left(J^* + i\mu^*\frac{\Gamma}{2}\right)\times\langle a^\dagger a\rangle + i\left(J^* - i\mu^*\frac{\Gamma}{2}\right)\langle b^\dagger b\rangle + iF\langle b\rangle, \quad \text{(A23)}$$

where $\mu = -p_b p_a^*$ and $\Gamma_i = \Gamma|p_i|^2$ with $i = a, b$. The symbols $\Re$ and $\Im$ indicate the real and imaginary parts, respectively.

The structure of the above equations explains why the significant enhancement reported in Ref. [62], which is based entirely on nonreciprocity, is only valid when the detuning is zero. This is because the nonreciprocity effect relies on cancellation of the second term in Eq. (A21), blocking backward energy flow. As a result, the laser field effectively "sees" only the charger and not the entire charger-battery system. Therefore, as the detuning deviates from zero, the benefits of nonreciprocity diminish, and in fact, the detuning negatively impacts the charging process.

3. Mixed approach

We now move to the crucial question of the paper: can the presence of an engineered shared reservoir enhance the optimal conventional charging process? Let us first consider adding the engineered shared reservoir to the charging process by setting $\Gamma \neq 0$. In this case, $E^S_{B,\mathrm{opt}}$ is obtained by optimizing E^S_B over the detuning in the stationary limit. We derive the optimal detuning to be again close to the built-in detuning Δ_{in}, with more convoluted corrections due to interactions with both local and shared reservoirs (see Appendix A 1). In this case, Δ_{opt} also depends on the interaction phase ϕ. As illustrated in Fig. 4, adding the shared reservoir does not provide a straightforward advantage over the optimal conventional charging process; however, there is another way to exploit the engineered shared reservoir, which we outline below.

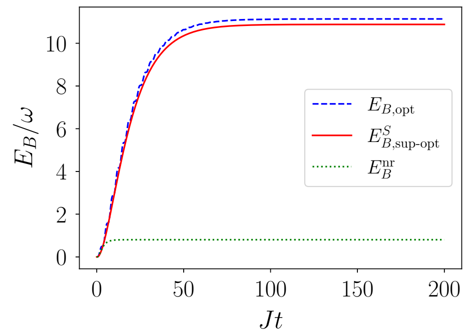

FIG. 4. Optimal energy of the battery in the conventional procedure (dashed blue line) and the shared-reservoir-assisted procedure (solid red line) vs Jt. The superscript S denotes the presence of the shared reservoir. Here, we have $|J| = 0.2$, $\kappa_a = 0.05$, and $\kappa_b = 0.01$, and for the shared-reservoir-assisted procedure, $\Gamma = 0.4$, $p_a = p_b = 1$, and $\phi = 0, \pi$. In both procedures, we selected the corresponding optimal detuning Δ_{opt}. The green dotted line, representing the nonreciprocal procedure at $\Delta = 0$ from Ref. [62], is plotted to highlight the significant impact of optimal detuning on the charging process.

4. Total Energy Comparison: Before and After Optimization

Typically, the charger-battery setup is considered from the perspective of the battery, which we control and can extract energy from, and which is more isolated than the charger: $\kappa_b < \kappa_a$; however, for the purpose of fully characterizing the model, we also analyze the effects of the optimization on the total energy and the energy of the charger, which can be extracted if operational control is established over these systems.

Replacing the coherent interaction J by the shared reservoir with dissipation rate Γ and then performing the optimization offers a significant change in both the overall and local energies of the system. In Fig. 5, the total energy of the system ξ^S in the steady state before (blue line) and after (red line) the optimization are illustrated. As can be seen, a significant increase is observed due to the optimization. Therefore, optimization preserves more energy in the charger-battery system against dissipation. From Eqs. (7)–(9) of the main text, we can observe the following relationships (since $\Gamma \gg \kappa_a, \kappa_b$):

$$E_{A,\text{sup-opt}} \approx \frac{F^2}{\kappa_a^2}, \quad E_{B,\text{sup-opt}} \approx \frac{F^2}{\kappa_a \kappa_b},$$
$$\text{and} \quad \xi_B^{\text{sup-opt}} \approx \frac{F^2(4\kappa_b + \kappa_a)}{\kappa_a^2 \kappa_b}.$$

These equations indicate that when $\kappa_a \to 0$, both $E_{A,\text{sup-opt}}$ and $\xi_{B,\text{sup-opt}}$ increase faster than $E_{B,\text{sup-opt}}$. Conversely, when $\kappa_b \to 0$, both $E_{B,\text{sup-opt}}$ and $\xi_{B,\text{sup-opt}}$ increase faster than $E_{A,\text{sup-opt}}$. Therefore, if the goal were solely to increase the total energy of the system, reducing the dissipation of the charger would be more effective; however, if we aim to boost both the total energy and the proportion of energy transferred to the battery, it is more advantageous to reduce the dissipation of the battery.

Moreover, looking at Eqs. (7)–(9) of the main text, we see that $E_{B,\text{sup-opt}}$ remains unchanged when κ_a and κ_b are swapped, whereas $E_{A,\text{sup-opt}}$ and $\xi_{B,\text{sup-opt}}$ do not. Since we aim not only to maximize energy transfer but also to improve the efficiency of the charging process—specifically, by increasing the amount of energy transferred while minimizing the energy left in the charger—it is more economical to decrease the battery dissipation rather than that of the charger.

In Fig. 6, we plot the energies of the charger, battery, and the entire system versus time for two cases: $\kappa_a = 0.05$ and $\kappa_b = 0.01$ [Fig. 6(a)], and $\kappa_a = 0.01$ and $\kappa_b = 0.05$ [Fig. 6(b)]. In both cases, we set $F = 0.1$ and $\Gamma = 0.4$; however, in general, when κ_b/κ_a exceeds a certain threshold, there is no advantage to superoptimal charging compared to optimal charging. But the beneficial aspect is that superoptimal charging is never worse than optimal charging (i.e., $\mathcal{G}^r_{A(B)} \geq 0$). In Fig. 7, we plot $\mathcal{G}^r_{A(B)}$ for two cases: $\kappa_a = 0.01$ [Fig. 7(a)] and $\kappa_a = 0.05$ [Fig. 7(b)]. In both cases, we set $J = 0.2$, $F = 0.1$ and $\Gamma = 0.4$.

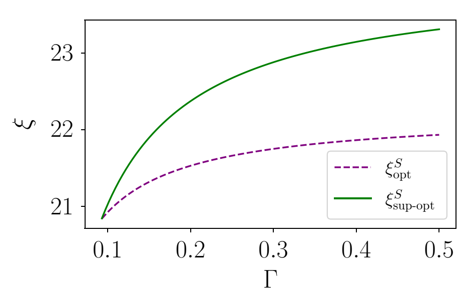

FIG. 5. Plots of ξ^S and ξ^S_{opt} vs Γ. For ξ^S, we have the optimized $p_a = p_b = 1$, and for ξ^S_{opt}, we have $p_a = (\kappa_a/\kappa_b)^{1/4}$ and $p_b = (\kappa_a/\kappa_b)^{-1/4}$. In both cases, we have $\Delta_{\mathrm{opt}} = 0$, $\kappa_a = 0.05$, and $\kappa_b = 0.01$.

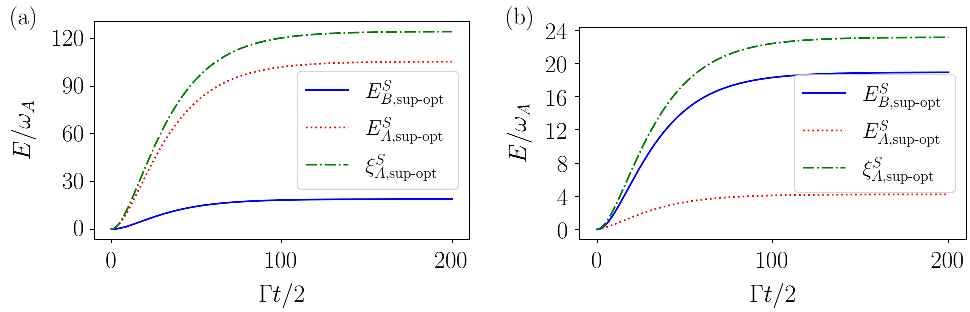

FIG. 6. Energies of the charger, battery, and the entire system vs time for two cases: (a) $\kappa_a = 0.05$ and $\kappa_b = 0.01$, and (b) $\kappa_a = 0.01$ and $\kappa_b = 0.05$. In both cases, we set $F = 0.1$ and $\Gamma = 0.4$.

5. Arbitrary Energy Transfer

The most significant result of the present paper is as follows. In conventional settings, whenever there is dissipation in the charging system, it becomes impossible to transfer an arbitrary amount of energy to the battery. The energy transfer is limited by dissipation, even if the battery itself is perfectly insulated from dissipation (i.e., $\kappa_b = 0$). Dissipation on the charger side alone ($\kappa_a \neq 0$) is sufficient to prevent unlimited energy transfer to the battery. This can be clearly shown using Eq. (4) of the main text by substituting $\Gamma = 0$ and Δ_{opt}:

$$E_{B,\text{opt}} = \frac{64F^2J^2}{(16J^2 - (\kappa_b - \kappa_a)^2)(\kappa_b + \kappa_a)^2}. \tag{A24}$$

Nonetheless, when operating in the nonzero detuning regime, we made a surprising discovery: this restriction can be lifted using reservoir engineering, by creating a dissipative interaction. The optimization freedom provided by reservoir engineering allows for this remarkable phenomenon, as demonstrated in Eq. (8) of the main text:

$$E_{B,\text{sup-opt}} = \frac{4F^2\Gamma^2}{\kappa_\alpha\kappa_b\left(2 + \frac{\kappa_\alpha}{\kappa_b}\right)}. \tag{A25}$$

By insulating only one of either the charger or the battery, it becomes possible to transfer an arbitrary amount of energy to the battery. This implies that as long as the battery remains connected to the charger, it continues to accumulate more energy over time. In other words, superoptimal charging *unlocks* the arbitrary energy transfer. In Fig. 8, we have plotted the energy of the battery versus time for both the conventional optimal scenario [Fig. 8(a)] and the superoptimal scenario [Fig. 8(b)]. In the conventional optimal scenario, we set $J = 0.2$, while in the superoptimal scenario, we use $\Delta = 0.4$. In both cases, we have fixed $F = 0.1$, $\kappa_\alpha = 0.05$, and $\kappa_b = 0$. We believe that this result holds significant promise for advancing quantum battery technology.

6. Positivity of $\mathcal{G}_B^r$

As illustrated in Fig. 3 (in the main text), to quantify the redistribution gap caused by the engineered shared reservoir, we also define the quantity $\mathcal{G}^r_{A(B)} \equiv E^S_{A(B),\text{sup-opt}} - E_{A(B),\text{opt}}$. As we are interested in the energy of the battery, we focus on

$$\mathcal{G}_B^r = 4\Gamma^2F^2\left(\frac{4}{(\kappa_a+\kappa_b)^2\left((\kappa_a-\kappa_b)^2 - 4\Gamma^2\right)} + \frac{1}{\kappa_a\kappa_b\left(2\Gamma + \sqrt{\kappa_a\kappa_b}\right)^2}\right)$$

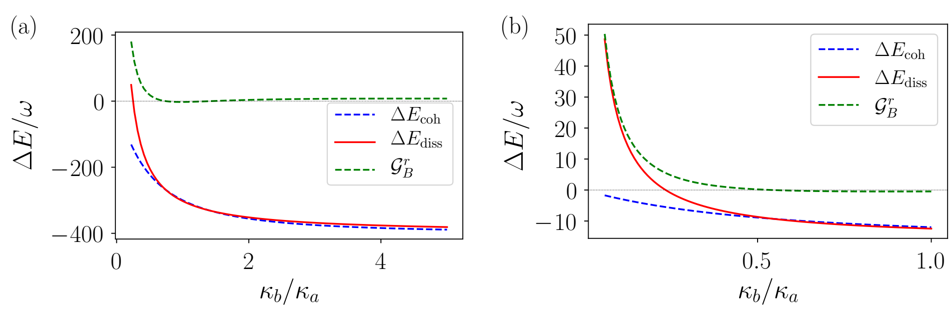

FIG. 7. Plots of ΔE_{coh}, ΔE_{diss}, and $\mathcal{G}^r_{A(B)}$ vs κ_b: (a) $\kappa_a = 0.01$ and (b) $\kappa_a = 0.05$. In both cases, we set $J = 0.2$ (for conventional optimal charging), $F = 0.1$, and $\Gamma = 0.4$ (for superoptimal charging).

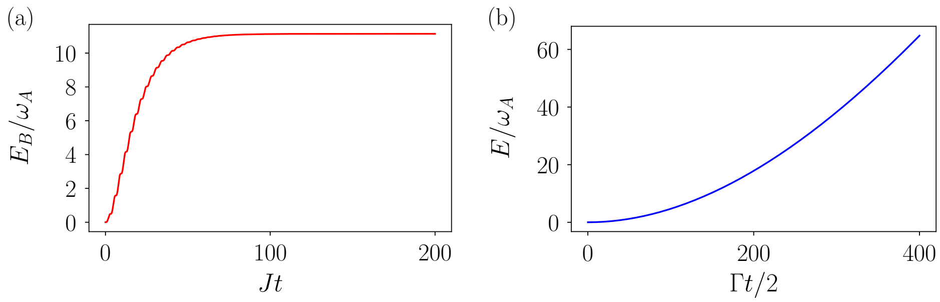

FIG. 8. Plots of energy of the battery vs time for different scenarios when the battery is perfectly insulated ($\kappa_b \approx 0$): (a) conventional optimal charging and (b) superoptimal charging. In both cases, we set $\kappa_a = 0.05$, $F = 0.1$, and $J = 0.2$ (for the conventional scenario), and $\Gamma = 0.4$ (for the shared-reservoir-assisted scenario).

and observe that in settings characterized by a significant difference in local dissipation rates κ_a and κ_b, this function is positive. This is attests to the charging scenarios in which we observe a guaranteed advantage of shared reservoir over coherent couplings.

7. Robustness against Detuning

The more we deviate from the optimal detuning, the worse the outcome. The interesting point to notice is that the conventional configuration is more robust against detuning deviation. The energy of the battery in the superoptimal configuration changes dramatically as we deviate from the optimal detuning, which is zero. In Fig. 9, we plot the energy of the battery for both the conventional [Fig. 9(a)] and superoptimal scenarios [Fig. 9(b)]. In both cases, we set $\kappa_a = 0.05$, $\kappa_b = 0.01$, $F = 0.1$, and $J = 0.2$ (for the conventional scenario), and $\Gamma = 0.4$ (for the shared-reservoir-assisted scenario). In both plots, the solid green lines represent the corresponding optimal detunings.

8. Varying Interaction Strengths

In the conventional scenario, by varying J, in Eq. (4) of the main text, two distinct peaks appear in the energy of the battery when $\Delta = \pm\sqrt{\Delta_{\text{in}}^2 - \kappa_\alpha^2/8}$, which aligns with the condition given by Eq. (5) of the main text. Additionally, increasing Γ can result in greater energy transfer, but this comes at the expense of longer charging times. This is because a higher Γ also leads to more dissipation, as evident from Eq. (8). To illustrate this, we provide two plots in Fig. 10 that confirm these observations.

Figure 10(a) illustrates the stationary E_B versus J and Δ in the conventional charging process, and Fig. 10(b) represents the stationary E_B in the superoptimal charging process as a function of Γ and Δ. In both cases, we set $F = 0.1$, $\kappa_\alpha = 0.05$, and $\kappa_b = 0.01$. Notably, the initial peak in Fig. 10(a) occurs because as J approaches zero, the optimal detuning also approaches zero. This peak happens at the cost of longer charging times; therefore, decreasing J in the conventional scenario is somehow equivalent to increasing Γ in the superoptimal charging process.

9. In defense of charger-battery setups

The advantages we have established are significant enough to address the motivational issues behind charger-battery charging settings. Specifically, Ref. [48] considered a separation of the charging setup into a charger, whose role is to receive energy from the laser drive, and a battery, whose role is to store the energy, coupled to the charger. The battery, while coupled coherently to the noisy

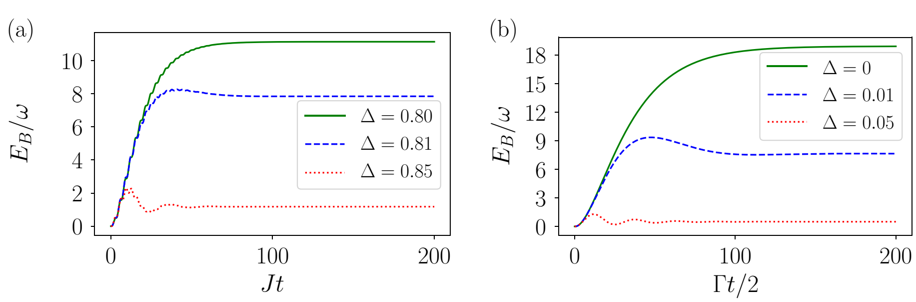

FIG. 9. Plots of the energy of the battery E_B vs time for various detunings: (a) conventional optimal charging and (b) superoptimal charging. In both cases, we set $\kappa_a = 0.05$, $\kappa_b = 0.01$, $F = 0.1$, and $J = 0.2$ (for conventional scenario), and $\Gamma = 0.4$ (for shared-reservoir assisted scenario). In both plots, the solid green lines represent the corresponding optimal detunings.

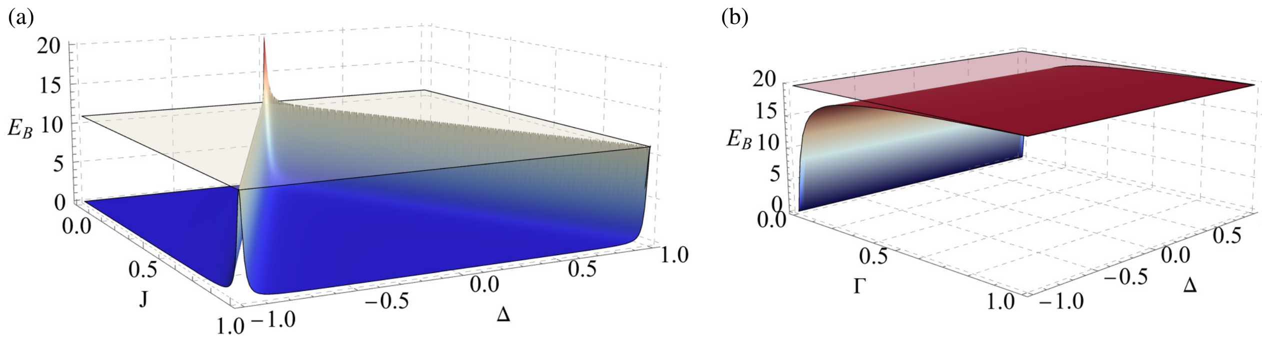

FIG. 10. Energy of the battery vs time for both scenarios: (a) conventional charging and (b) superoptimal charging. In both cases, we set $\kappa_a = 0.05$, $\kappa_b = 0.01$, $F = 0.1$, and $J = 0.2$ (for the conventional scenario), and $\Gamma = 0.4$ (for the superoptimal scenario).

charger, can be much more isolated in experimental implementations, and therefore experience much smaller energy dissipation. Nonetheless, in Ref. [70], the authors pointed to the lack of operational benefit of using this extended setting compared to the simple model of a battery interacting directly with the laser field.

This problem, and the role of superoptimal charging in solving it, is illustrated in Fig. 11. Three charging scenarios are presented there: direct coupling of the battery to the laser [Fig. 11(a)], a charger-mediated setting with the charger coherently coupled to the battery [Fig. 11(b)], and a charger-mediated setting with the charger dissipatively coupled to the battery [Fig. 11(c)]. We ask the following question: can we obtain higher energies in the stationary state of the battery if we include a charger to intermediate between the laser and the battery? In this procedure, we keep the dissipation rate κ of the party interacting with laser constant, and we allow for smaller values of the dissipation rate κ_b of the battery in the extended scenario to account for its better isolation from the surroundings.

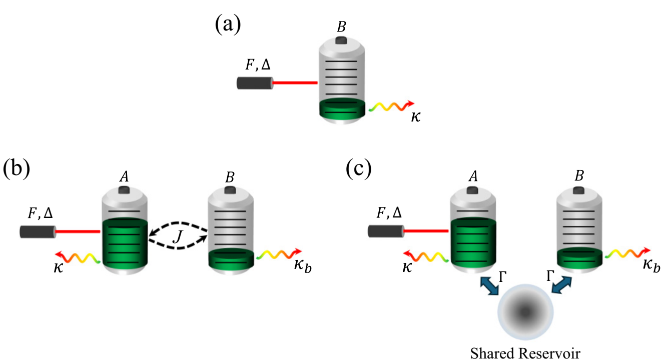

FIG. 11. Three charging scenarios: (a) direct coupling of the battery to the laser, (b) charger-mediated setting, with charger coherently coupled to the battery, and (c) charger-mediated setting, with charger dissipatively coupled to the battery. In (b),(c), the presence of system A (charger) isolates the battery and assures smaller dissipation $\kappa_b < \kappa$.

We compare stationary energies achieved with the extended scenarios of Fig. 11(b) E_B [given by Eqs. (4) and (5) of the main text] and Fig. 11(c) $E^S_{B,\text{sup-opt}}$ (given by Eq. (8) of the main text) with the stationary energy of the scenario of Fig. 11(a):

$$E_{\text{single-batt}} = \frac{4F^2}{\kappa_a^2}, \tag{A26}$$

and obtain

$$\Delta E_{\text{coh}} \equiv E_{B,\text{opt}} - E_{\text{single-batt}} = 4F^2\left(\frac{4J^2}{(\kappa+\kappa_b)^2\left(4J^2-(\kappa-\kappa_b)^2\right)} - \frac{1}{\kappa^2}\right), \tag{A27}$$

$$\Delta E_{\text{diss}} \equiv E^S_{B,\text{sup-opt}} - E_{\text{single-batt}} = \frac{4F^2\left(\frac{\Gamma^2\kappa}{\kappa_b\left(2\Gamma+\sqrt{\kappa}\sqrt{\kappa_b}\right)^2} - 1\right)}{\kappa^2}. \tag{A28}$$

We plot these functions for typical parameter settings in Fig. 12. As shown, with sufficient isolation of the battery (i.e., sufficiently small κ_b), the superoptimal charging process is significantly more efficient than the direct charging scenario. In fact, in the limit of perfect isolation of the battery, the superoptimal charging allows for unbounded values of energy stored $\lim_{\kappa_b\to 0}\Delta E_{\text{diss}} = \infty$, while the energy in the coherent setting is bounded: $\lim_{\kappa_b\to 0}\Delta E_{\text{coh}} = 4F^2/(4J^2-\kappa^2)$. The charger-mediated setting with coherent coupling is beneficial only in the regime of extremely small κ_b; therefore, the extension of the noisy single-battery system via the superoptimal setting effectively allows for creating a charged battery system with energy not bounded by the dissipation on the original charger. As can be seen from Fig. 12 in general, when κ_b/κ_a exceeds a certain threshold, there is no advantage to superoptimal charging compared to optimal charging;

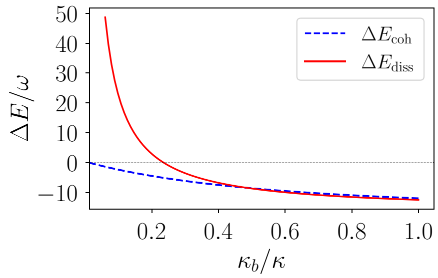

FIG. 12. Advantage in stationary energy of the battery B in the extended scenarios [corresponding to Figs. 11(b) and 11(c)] compared to the single-battery scenario [Fig. 11(a)], expressed through $\Delta E_{\rm coh}$ and $\Delta E_{\rm diss}$, respectively, for various dissipation rates κ_b. For scenario (a), we choose $F = 0.1$; for (b), we have $F = 0.1, J = 0.2$, and $\Gamma = 0$; and for (c), we select $F = 0.1, J = 0$, and $\Gamma = 0.4$, and the optimized values $p_a = (\kappa_a/\kappa_b)^{1/4}$ and $p_b = (\kappa_a/\kappa_b)^{-1/4}$. In all scenarios, we choose $\kappa = 0.05$ and the corresponding optimal detuning $\Delta_{\rm opt}$. We have $\lim_{\kappa_b\to 0}\Delta E_{\rm diss} = \infty$ and $\Delta E_{\rm coh}(0) = 0.016$.

however, the important point is that superoptimal charging is never worse than optimal charging, i.e., $\mathcal{G}^r_{A(B)} \geq 0$ (see Appendix A 4 for further details).

We conclude the characterization of superoptimal charging with a remark about the transient behavior of this charging method. The effective coupling strength of the dissipative interaction depends entirely on the value of Γ [see Eq. (6) of the main text]. Therefore, while the superoptimal scenario for more isolated batteries relies on reduced Γ_b (as implied by reduced κ_b via $y = \sqrt{\kappa_a/\kappa_b}$), the limit $\lim_{\kappa_b\to 0}$ does not impose divergent times for reaching a given value of the energy of the battery. Consequently, the advantage of superoptimal charging over the single-battery setting can be observed within the same time scales, and it therefore offers a significant practically achievable boost in capacity of quantum batteries.

[1] L. Wang and B. Li, Thermal logic gates: Computation with phonons, Phys. Rev. Lett. **99**, 177208 (2007).
[2] K. Joulain, J. Drevillon, Y. Ezzahri, and J. Ordonez-Miranda, Quantum thermal transistor, Phys. Rev. Lett. **116**, 200601 (2016).
[3] A. H. A. Malavazi, B. Ahmadi, P. Mazurek, and A. Mandarino, Detuning effects for heat-current control in quantum thermal devices, Phys. Rev. E **109**, 064146 (2024).
[4] F. Campaioli, S. Gherardini, J. Q. Quach, M. Polini, and G. M. Andolina, Colloquium: Quantum batteries, Rev. Mod. Phys. **96**, 031001 (2024).
[5] S.-Y. Bai and J.-H. An, Floquet engineering to reactivate a dissipative quantum battery, Phys. Rev. A **102**, 060201 (2020).
[6] M. Łobejko, T. Biswas, P. Mazurek, and M. Horodecki, Catalytic advantage in Otto-like two-stroke quantum engines, Phys. Rev. Lett. **132**, 260403 (2024).
[7] D. Ferraro, M. Campisi, G. M. Andolina, V. Pellegrini, and M. Polini, High-power collective charging of a solid-state quantum battery, Phys. Rev. Lett. **120**, 117702 (2018).
[8] G. M. Andolina, M. Keck, A. Mari, M. Campisi, V. Giovannetti, and M. Polini, Extractable work, the role of correlations, and asymptotic freedom in quantum batteries, Phys. Rev. Lett. **122**, 047702 (2019).
[9] F.-Q. Dou and F.-M. Yang, Superconducting transmon qubit-resonator quantum battery, Phys. Rev. A **107**, 023725 (2023).
[10] O. A. D. Molitor, A. H. A. Malavazi, R. D. Baldijão, A. C. Orthey, I. L. Paiva, and P. R. Dieguez, Quantum switch instabilities with an open control, Commun. Phys. **7**, 373 (2024).
[11] R. Alicki and M. Fannes, Entanglement boost for extractable work from ensembles of quantum batteries, Phys. Rev. E **87**, 042123 (2013).
[12] R. Salvia, M. Perarnau-Llobet, G. Haack, N. Brunner, and S. Nimmrichter, Quantum advantage in charging cavity and spin batteries by repeated interactions, Phys. Rev. Res. **5**, 013155 (2023).
[13] R. R. Rodríguez, B. Ahmadi, G. Suárez, P. Mazurek, S. Barzanjeh, and P. Horodecki, Optimal quantum control of charging quantum batteries, New J. Phys. **26**, 043004 (2024).
[14] F. Mazzoncini, V. Cavina, G. M. Andolina, P. A. Erdman, and V. Giovannetti, Optimal control methods for quantum batteries, Phys. Rev. A **107**, 032218 (2023).
[15] F. H. Kamin, S. Salimi, and M. B. Arjmandi, Steady-state charging of quantum batteries via dissipative ancillas, Phys. Rev. A **109**, 022226 (2024).
[16] F. Kamin, F. Tabesh, S. Salimi, F. Kheirandish, and A. C. Santos, Non-Markovian effects on charging and self-discharging process of quantum batteries, New J. Phys. **22**, 083007 (2020).
[17] F. C. Binder, S. Vinjanampathy, K. Modi, and J. Goold, Quantacell: Powerful charging of quantum batteries, New J. Phys. **17**, 075015 (2015).
[18] R. R. Rodríguez, B. Ahmadi, P. Mazurek, S. Barzanjeh, R. Alicki, and P. Horodecki, Catalysis in charging quantum batteries, Phys. Rev. A **107**, 042419 (2023).
[19] W.-L. Song, H.-B. Liu, B. Zhou, W.-L. Yang, and J.-H. An, Remote charging and degradation suppression for the quantum battery, Phys. Rev. Lett. **132**, 090401 (2024).
[20] A. H. A. Malavazi, R. Sagar, B. Ahmadi, and P. R. Dieguez, Weak measurement-based protocol for ergotropy protection in open quantum batteries, arXiv:2411.16633.
[21] G. Zhu, Y. Chen, Y. Hasegawa, and P. Xue, Charging quantum batteries via indefinite causal order: Theory and experiment, Phys. Rev. Lett. **131**, 240401 (2023).
[22] Z.-G. Lu, G. Tian, X.-Y. Lü, and C. Shang, Topological quantum batteries, arXiv:2405.03675.
[23] H.-L. Shi, S. Ding, Q.-K. Wan, X.-H. Wang, and W.-L. Yang, Entanglement, coherence, and extractable work in quantum batteries, Phys. Rev. Lett. **129**, 130602 (2022).
[24] M. B. Arjmandi, A. Shokri, E. Faizi, and H. Mohammadi, Performance of quantum batteries with correlated and uncorrelated chargers, Phys. Rev. A **106**, 062609 (2022).
[25] A. Crescente, D. Ferraro, M. Carrega, and M. Sassetti, Enhancing coherent energy transfer between quantum devices via a mediator, Phys. Rev. Res. **4**, 033216 (2022).

[26] J. Q. Quach, K. E. McGhee, L. Ganzer, D. M. Rouse, B. W. Lovett, E. M. Gauger, J. Keeling, G. Cerullo, D. G. Lidzey, and T. Virgili, Superabsorption in an organic microcavity: Toward a quantum battery, Sci. Adv. **8**, 3160 (2022).
[27] A. Glicenstein, G. Ferioli, A. Browaeys, and I. Ferrier-Barbut, From superradiance to subradiance: Exploring the many-body Dicke ladder, Opt. Lett. **47**, 1541 (2022).
[28] F. Barra, K. V. Hovhannisyan, and A. Imparato, Quantum batteries at the verge of a phase transition, New J. Phys. **24**, 015003 (2022).
[29] J. Carrasco, J. R. Maze, C. Hermann-Avigliano, and F. Barra, Collective enhancement in dissipative quantum batteries, Phys. Rev. E **105**, 064119 (2022).
[30] J.-Y. Gyhm, D. Šafránek, and D. Rosa, Quantum charging advantage cannot be extensive without global operations, Phys. Rev. Lett. **128**, 140501 (2022).
[31] S. Mondal and S. Bhattacharjee, Periodically driven many-body quantum battery, Phys. Rev. E **105**, 044125 (2022).
[32] G. Gemme, G. M. Andolina, F. M. D. Pellegrino, M. Sassetti, and D. Ferraro, Off-resonant Dicke quantum battery: Charging by virtual photons, Batteries **9**, 197 (2023).
[33] F. Centrone, L. Mancino, and M. Paternostro, Charging batteries with quantum squeezing, Phys. Rev. A **108**, 052213 (2023).
[34] F.-Q. Dou, Y.-J. Wang, and J.-A. Sun, Highly efficient charging and discharging of three-level quantum batteries through shortcuts to adiabaticity, Front. Phys. **17**, 31503 (2022).
[35] J.-s. Yan and J. Jing, Charging by quantum measurement, Phys. Rev. Appl. **19**, 064069 (2023).
[36] O. Abah, G. De Chiara, M. Paternostro, and R. Puebla, Harnessing nonadiabatic excitations promoted by a quantum critical point: Quantum battery and spin squeezing, Phys. Rev. Res. **4**, L022017 (2022).
[37] M.-L. Song, L.-J. Li, X.-K. Song, L. Ye, and D. Wang, Environment-mediated entropic uncertainty in charging quantum batteries, Phys. Rev. E **106**, 054107 (2022).
[38] V. Shaghaghi, V. Singh, G. Benenti, and D. Rosa, Micromasers as quantum batteries, Quantum Sci. Technol. **7**, 04LT01 (2022).
[39] V. Shaghaghi, V. Singh, M. Carrega, D. Rosa, and G. Benenti, Lossy micromaser battery: Almost pure states in the Jaynes–Cummings regime, Entropy **25**, 430 (2023).
[40] D.-L. Yang, F.-M. Yang, and F.-Q. Dou, Three-level Dicke quantum battery, Phys. Rev. B **109**, 235432 (2024).
[41] P. Bakhshinezhad, B. R. Jablonski, F. C. Binder, and N. Friis, Trade-offs between precision and fluctuations in charging finite-dimensional quantum batteries, Phys. Rev. E **109**, 014131 (2024).
[42] S. Imai, O. Gühne, and S. Nimmrichter, Work fluctuations and entanglement in quantum batteries, Phys. Rev. A **107**, 022215 (2023).
[43] F. Barra, Efficiency fluctuations in a quantum battery charged by a repeated interaction process, Entropy **24**, 820 (2022).
[44] X. Huang, K. Wang, L. Xiao, L. Gao, H. Lin, and P. Xue, Demonstration of the charging progress of quantum batteries, Phys. Rev. A **107**, L030201 (2023).
[45] G. Gemme, M. Grossi, D. Ferraro, S. Vallecorsa, and M. Sassetti, IBM quantum platforms: A quantum battery perspective, Batteries **8**, 43 (2022).
[46] D. Morrone, M. A. C. Rossi, A. Smirne, and M. G. Genoni, Charging a quantum battery in a non-Markovian environment: A collisional model approach, Quantum Sci. Technol. **8**, 035007 (2023).
[47] A. Crescente, D. Ferraro, M. Carrega, and M. Sassetti, Analytically solvable model for qubit-mediated energy transfer between quantum batteries, Entropy **25**, 758 (2023).
[48] D. Farina, G. M. Andolina, A. Mari, M. Polini, and V. Giovannetti, Charger-mediated energy transfer for quantum batteries: An open-system approach, Phys. Rev. B **99**, 035421 (2019).
[49] J. F. Poyatos, J. I. Cirac, and P. Zoller, Quantum reservoir engineering with laser cooled trapped ions, Phys. Rev. Lett. **77**, 4728 (1996).
[50] A. Metelmann and A. A. Clerk, Quantum-limited amplification via reservoir engineering, Phys. Rev. Lett. **112**, 133904 (2014).
[51] A. Metelmann and A. A. Clerk, Nonreciprocal photon transmission and amplification via reservoir engineering, Phys. Rev. X **5**, 021025 (2015).
[52] L. D. Toth, N. R. Bernier, A. Nunnenkamp, A. K. Feofanov, and T. J. Kippenberg, A dissipative quantum reservoir for microwave light using a mechanical oscillator, Nat. Phys. **13**, 787 (2017).
[53] S. Barzanjeh, M. Wulf, M. Peruzzo, M. Kalaee, P. B. Dieterle, O. Painter, and J. M. Fink, Mechanical on-chip microwave circulator, Nat. Commun. **8**, 953 (2017).
[54] J. Kerckhoff, K. Lalumière, B. J. Chapman, A. Blais, and K. W. Lehnert, On-chip superconducting microwave circulator from synthetic rotation, Phys. Rev. Appl. **4**, 034002 (2015).
[55] B. J. Chapman, E. I. Rosenthal, J. Kerckhoff, B. A. Moores, L. R. Vale, J. A. B. Mates, G. C. Hilton, K. Lalumière, A. Blais, and K. W. Lehnert, Widely tunable on-chip microwave circulator for superconducting quantum circuits, Phys. Rev. X **7**, 041043 (2017).
[56] M. Kim, A. Tabesh, T. Zegray, S. Barzanjeh, and C.-M. Hu, Nonreciprocity in cavity magnonics at millikelvin temperature, J. Appl. Phys. **135**, 063904 (2024).
[57] S. Barzanjeh, M. Aquilina, and A. Xuereb, Manipulating the flow of thermal noise in quantum devices, Phys. Rev. Lett. **120**, 060601 (2018).
[58] F. Verstraete, M. M. Wolf, and J. Ignacio Cirac, Quantum computation and quantum-state engineering driven by dissipation, Nat. Phys. **5**, 633 (2009).
[59] J. T. Barreiro, M. Müller, P. Schindler, D. Nigg, T. Monz, M. Chwalla, M. Hennrich, C. F. Roos, P. Zoller, and R. Blatt, An open-system quantum simulator with trapped ions, Nature **470**, 486 (2011).
[60] K. W. Murch, S. Weber, C. Macklin, and I. Siddiqi, Observing single quantum trajectories of a superconducting quantum bit, Nature **502**, 211 (2013).
[61] H. Krauter, C. A. Muschik, K. Jensen, W. Wasilewski, J. M. Petersen, J. I. Cirac, and E. S. Polzik, Entanglement generated by dissipation and steady state entanglement of two macroscopic objects, Phys. Rev. Lett. **107**, 080503 (2011).

[62] B. Ahmadi, P. Mazurek, P. Horodecki, and S. Barzanjeh, Nonreciprocal quantum batteries, Phys. Rev. Lett. **132**, 210402 (2024).

[63] H.-P. Breuer and F. Petruccione *et al.*, *The Theory of Open Quantum Systems* (Oxford University, Oxford, 2007).

[64] A. F. Kockum, G. Johansson, and F. Nori, Decoherence-free interaction between giant atoms in waveguide quantum electrodynamics, Phys. Rev. Lett. **120**, 140404 (2018).

[65] D. Chang, A. H. Safavi-Naeini, M. Hafezi, and O. Painter, Slowing and stopping light using an optomechanical crystal array, New J. Phys. **13**, 023003 (2011).

[66] R. Alicki, The quantum open system as a model of the heat engine, J. Phys. A: Math. Gen. **12**, L103 (1979).

[67] A. Kossakowski, On quantum statistical mechanics of non-Hamiltonian systems, Rep. Math. Phys. **3**, 247 (1972).

[68] A. E. Allahverdyan, R. Balian, and T. M. Nieuwenhuizen, Maximal work extraction from finite quantum systems, Europhys. Lett. **67**, 565 (2004).

[69] R. R. Puri, *Mathematical Methods of Quantum Optics* (Springer Berlin, Heidelberg, 2001).

[70] K. Gangwar and A. Pathak, Coherently driven quantum harmonic oscillator battery, Adv. Quantum Technol. **7**, 2400069 (2024).